Numerical experiments in idealized glacier topographies

Case study of the impact of the mesh resolution on the prediction of the grounding line position

Ruben Espeleta Bolivar
Advisor: Dr. Cruz García Molina

[1]Institut des geosciences de l'environnement

Presented in the partial fulfillment of the requirements for the degree of Master applied mechanics

Institut
des géosciences
de l'environnement

Content

Institut des géosciences de l'environnement

What is a glacier?

Glaciers can be defined as a mass of ice that accumulates from snow and flows downwards from a few hundreds of meters per year and up to 15 km per year.

Institut
des géosciences
de l'environnement

What is a glacier?

Glaciers can be defined as a mass of ice that accumulates from snow and flows downwards from a few hundreds of meters per year and up to 15 km per year.

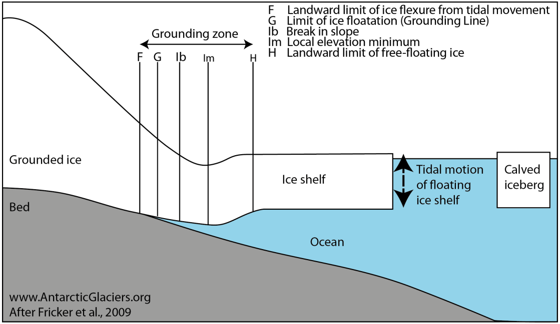

Figure: Schema of a tributary glacier where we can observe the different parts denoting the grounding zone. Adapted from Fricker et al. (2009).

Importance of understanding the dynamics of glaciers

- The rate of present-day sea-level rise has increased in recent decades and it is expected to continue increasing in coming decades and centuries (Clark et al., 2015).

Importance of understanding the dynamics of glaciers

- The rate of present-day sea-level rise has increased in recent decades and it is expected to continue increasing in coming decades and centuries (Clark et al., 2015).
- Mass loss from glaciers is strongly linked to changes in the ice shelves and their grounding lines (Brunt et al., 2010; Pritchard et al., 2012).

Importance of understanding the dynamics of glaciers

- The rate of present-day sea-level rise has increased in recent decades and it is expected to continue increasing in coming decades and centuries (Clark et al., 2015).
- Mass loss from glaciers is strongly linked to changes in the ice shelves and their grounding lines (Brunt et al., 2010; Pritchard et al., 2012).
- Ice thinning and rising sea levels can cause grounding line to retreat while thickening or declining sea levels can cause an advance (Friedl et al., 2020).

Institut des géosciences de l'environnement

Glacier flow

Figure: Glaciers behave as a very viscous fluid for time scales between a few years to a few thousands of years.

Governing equations

The plastic lower ice of the glacier can flow like a very viscous fluid. The incompressibility condition leads to:

$$\nabla \cdot u = 0. \tag{1}$$

Institut des géosciences de l'environnement

Governing equations

The plastic lower ice of the glacier can flow like a very viscous fluid. The incompressibility condition leads to:

$$\nabla \cdot u = 0. \tag{1}$$

For ice flow, the acceleration term can be neglected in the Navier-Stokes equations (Hutter, 1982). Therefore:

$$-\nabla \cdot p + \nabla \cdot (\eta(\nabla \cdot u + (\nabla \cdot u)^T)) + \rho g = 0. \tag{2}$$

Where η is the viscosity and g is the gravity.

IGE
Institut des géosciences de l'environnement

Governing equations

The plastic lower ice of the glacier can flow like a very viscous fluid. The incompressibility condition leads to:

$$\nabla \cdot u = 0. \tag{1}$$

For ice flow, the acceleration term can be neglected in the Navier-Stokes equations (Hutter, 1982). Therefore:

$$-\nabla \cdot p + \nabla \cdot (\eta(\nabla \cdot u + (\nabla \cdot u)^T)) + \rho g = 0. \tag{2}$$

Where η is the viscosity and g is the gravity. Letting σ denote the stress tensor and pressure p is the mean normal stress, and the strain rate tensor ϵ_e, related by:

$$\sigma = 2\eta\epsilon_e - pI = \eta \cdot (\nabla \cdot u + (\nabla \cdot u)^T) - pI. \tag{3}$$

Where I is the identity tensor. Together, these two last mathematical equations are called the full-stokes model.

The flow law

The most commonly used flow law for ice is Glen's flow law, named after John W. Glen upon whose experiments it is based Glen (1958). This equation was originally written in the form:

$$\dot{\epsilon_e} = (\frac{\sigma_e}{B})^n; \tag{4}$$

Institut
des géosciences
de l'environnement

The flow law

The most commonly used flow law for ice is Glen's flow law, named after John W. Glen upon whose experiments it is based Glen (1958). This equation was originally written in the form:

$$\dot{\epsilon_e} = (\frac{\sigma_e}{B})^n; \tag{4}$$

where B is a viscosity parameter that increases as the ice becomes stiffer, and n is an empirically determined constant, and n=3. An alternative form of the flow law that is commonly used, and that can be used, is:

$$\dot{\epsilon_e} = A{\sigma_e}^n \tag{5}$$

Institut
des géosciences
de l'environnement

The flow law

The most commonly used flow law for ice is Glen's flow law, named after John W. Glen upon whose experiments it is based Glen (1958). This equation was originally written in the form:

$$\dot{\epsilon_e} = (\frac{\sigma_e}{B})^n; \tag{4}$$

where B is a viscosity parameter that increases as the ice becomes stiffer, and n is an empirically determined constant, and n=3. An alternative form of the flow law that is commonly used, and that can be used, is:

$$\dot{\epsilon_e} = A{\sigma_e}^n \tag{5}$$

A is called the rate factor. B is normally given in Mpa $\text{yr}^{\frac{1}{n}}$ while A is in MPa^{-n} yr $^{-1}$ or MPa^{-n} s $^{-1}$.

Institut des géosciences de l'environnement

Boundary conditions and time evolution

- Ice in contact with the bedrock: Weertman sliding law (Weertman, 1974):

$$u_b = C{\tau_b}^m; \tag{6}$$

IGE
Institut
des géosciences
de l'environnement

Boundary conditions and time evolution

- Ice in contact with the bedrock: Weertman sliding law (Weertman, 1974):

$$u_b = C{\tau_b}^m; \tag{6}$$

- The ice surface is assummed stress free $\sigma.n = 0$ and ice base at z_s and z_b behave as free surfaces according to:

$$\frac{\delta z_i}{\delta t} + u_i \frac{\delta z_i}{\delta x} + v_i \frac{\delta z_i}{\delta y} = w_i + a_i; \tag{7}$$

  where a_i is the accumulation $(a_i > 0)$ or ablation $(a_i < 0)$ in meter ice equivalent per year, and $i =$ surface or base, respectively.

IGE Institut des géosciences de l'environnement

Boundary conditions and time evolution

- Ice in contact with the bedrock: Weertman sliding law (Weertman, 1974):

$$u_b = C{\tau_b}^m; \tag{6}$$

- The ice surface is assummed stress free $\sigma.n = 0$ and ice base at z_s and z_b behave as free surfaces according to:

$$\frac{\delta z_i}{\delta t} + u_i \frac{\delta z_i}{\delta x} + v_i \frac{\delta z_i}{\delta y} = w_i + a_i; \tag{7}$$

  where a_i is the accumulation $(a_i > 0)$ or ablation $(a_i < 0)$ in meter ice equivalent per year, and $i =$ surface or base, respectively.

- By vertical integration of the incompressibility condition, w can be eliminated:

$$\frac{\delta H}{\delta t} + \frac{\delta H\bar{u}}{\delta x} + \frac{\delta H\bar{v}}{\delta y} = a_s - a_b; \tag{8}$$

  Where $\bar{u}$ and $\bar{v}$ are the vertically integrated horizontal velocities.

IGE
Institut des géosciences de l'environnement

Boundary conditions and time evolution

- Ice in contact with the bedrock: Weertman sliding law (Weertman, 1974):

$$u_b = C{\tau_b}^m; \tag{6}$$

- The ice surface is assummed stress free $\sigma.n = 0$ and ice base at z_s and z_b behave as free surfaces according to:

$$\frac{\delta z_i}{\delta t} + u_i \frac{\delta z_i}{\delta x} + v_i \frac{\delta z_i}{\delta y} = w_i + a_i; \tag{7}$$

  where a_i is the accumulation $(a_i > 0)$ or ablation $(a_i < 0)$ in meter ice equivalent per year, and $i =$ surface or base, respectively.
- By vertical integration of the incompressibility condition, w can be eliminated:

$$\frac{\delta H}{\delta t} + \frac{\delta H\bar{u}}{\delta x} + \frac{\delta H\bar{v}}{\delta y} = a_s - a_b; \tag{8}$$

  Where $\bar{u}$ and $\bar{v}$ are the vertically integrated horizontal velocities.
- For the ice-ocean interface, the ice flux out of the domain will be fixed as the calving rate.

IGE
Institut des géosciences de l'environnement

Shallow shelf approximation

SSA approximation has been derived by dimensional analysis based on a small aspect ratio between vertical and longitudinal lenght of the ice shelf The conservation of momentum simplifies to:

$$\nabla_h \cdot (2\bar{\eta}(\dot{\epsilon_h} I)) = \rho g H \nabla_h \cdot z_s; \tag{9}$$

Where the subscript h represents the components in the x-y plane and $\bar{\eta}$ the vertically integrated viscosity. The effective strain rate simplifies to:

$$\dot{\epsilon_h} = \sqrt{\frac{\delta u}{\delta x}^2 + \frac{\delta v}{\delta y}^2 + \frac{\delta u}{\delta x}\frac{\delta v}{\delta y} + \frac{1}{4}(\frac{\delta u}{\delta y} + \frac{\delta v}{\delta y})^2}; \tag{10}$$

IGE Institut des géosciences de l'environnement

Grounding line dynamics and stability

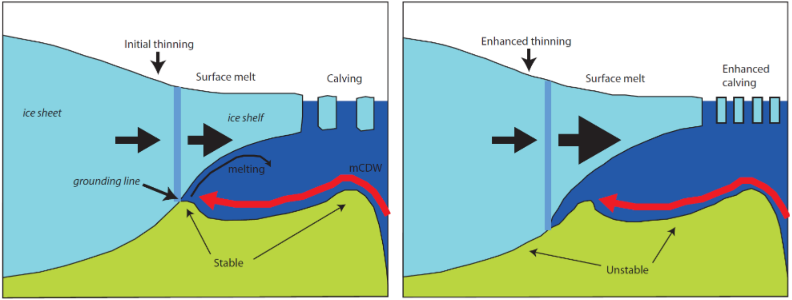

Figure: Schematic representation of the marine ice sheet instability with an initial stable grounding line position (left hand side) and unstable grounding line position after the incursion of warm circumpolar deep water below the ice shelf. Adapted from Hanna et al. (2013).

IGE
Institut
des géosciences
de l'environnement

Process of modelling

The physical phenomena that impacts the dynamics of the glaciers can be represented using mathematical models that implement partial differential equations, which can then be discretized to be solved using numerical methods.

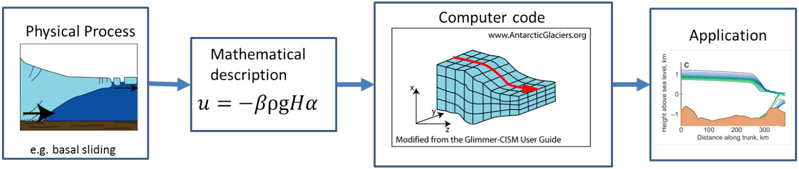

Figure: Process of modelling, starting with a physical phenomena which can be represented mathematically in a physical model than can then be discretized to solve numerically.

Institut des géosciences de l'environnement

- Numerical technique to calculate approximate solutions to differential equations problems.

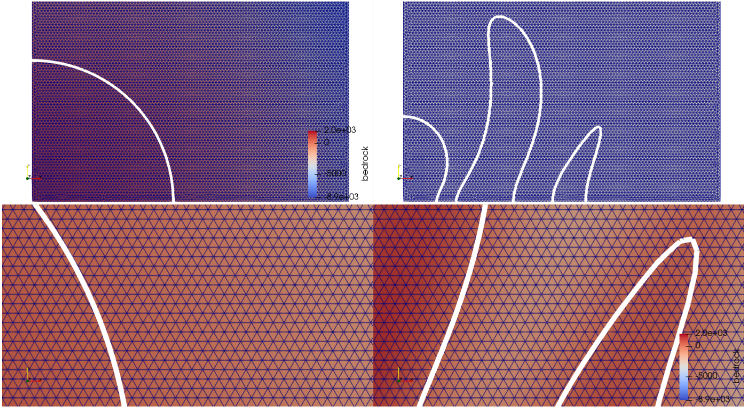

Figure: Discretization of the glacier domain using finite elements.

Elmer/Ice finite element method

- Open source finite element code, mainly developed in Grenoble and Helsinki. Still being developed and there are many contributors

Institut
des géosciences
de l'environnement

Elmer/Ice finite element method

- Open source finite element code, mainly developed in Grenoble and Helsinki. Still being developed and there are many contributors
- The ice sheet/ice flow model Elmer/Ice is based on Elmer and includes developments related to glaciological problems. It includes a large number of dedicated solvers and users functions.

Elmer/Ice finite element method

- Open source finite element code, mainly developed in Grenoble and Helsinki. Still being developed and there are many contributors
- The ice sheet/ice flow model Elmer/Ice is based on Elmer and includes developments related to glaciological problems. It includes a large number of dedicated solvers and users functions.
- Elmer/Ice solves the Stokes equations and it includes solvers for the approximations of the Stokes equations, namely shallow shelf and shallow ice approximations.

Institut des géosciences de l'environnement

- The intercomparison project (https://github.com/JRowanJordan/Calving is intended to develop models to explore calving, ice damage, and glacier dynamics leading to recommendations for improved calving laws in ice sheet models.

Institut des géosciences de l'environnement

Calving intercomparison project

- The intercomparison project (https://github.com/JRowanJordan/Calving is intended to develop models to explore calving, ice damage, and glacier dynamics leading to recommendations for improved calving laws in ice sheet models.
- The objective is to develop a model based on the topographies proposed by the CalvingMIP project to study the grounding line position for different resolutions.

Institut des géosciences de l'environnement

Cone domain

The idealised experimental domain comprise a simple, symmetrically circular domain. This first idealized model consists of a circular bedrock configuration (Figure 6) given by:

$$Bed_0 = Bc - (Bc - Bl)\frac{|x^2 + y^2|}{r^2}; \tag{11}$$

Where r=800x10^3m, Bc=0.9 x 10^3m, and Bl=-2 x 10^3m.

Institut des géosciences de l'environnement

Cone domain

The idealised experimental domain comprise a simple, symmetrically circular domain. This first idealized model consists of a circular bedrock configuration (Figure 6) given by:

$$Bed_0 = Bc - (Bc - Bl)\frac{|x^2 + y^2|}{r^2}; \tag{11}$$

Where r=800x10^3m, Bc=0.9 x 10^3m, and Bl=-2 x 10^3m.

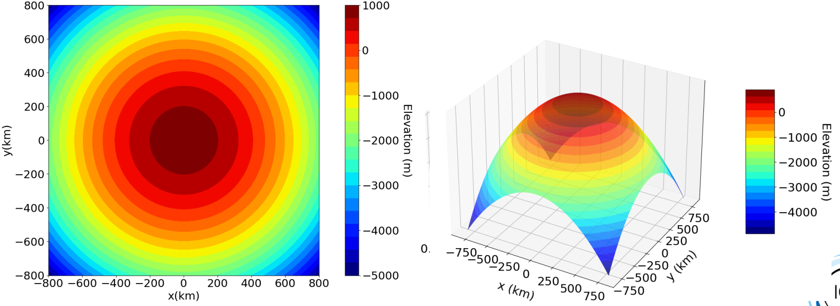

Figure: Circular bedrock topography. On the left side top view and on the right side, lateral view.

Experimental profiles

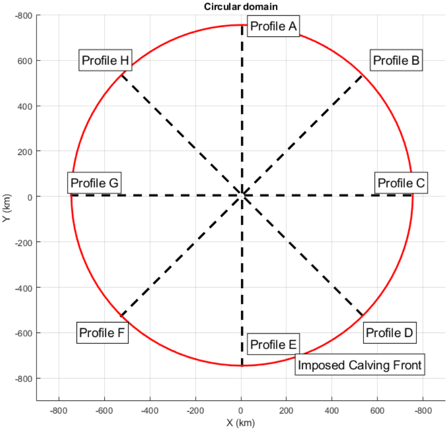

Figure: Circular domain experimental profiles as well as the initial imposed calving front position. Adapted from CalvingMIP inter-comparison project.

The Thule bedrock configuration is shown in Figure 8 and is given by:

$$\theta = arctan2(y, x); \tag{12}$$

$$l = r - cos(2\theta)\frac{r}{2}; \tag{13}$$

$$Bed_0 = Bc - (Bc - Bl)\frac{|x^2 + y^2|}{r^2}; \tag{14}$$

$$Bed = Bacos(3\pi\frac{\sqrt{x^2 + y^2}}{l}) + Bed_0; \tag{15}$$

With r=800 x $10^3 m$, Bc=0,9 x $10^3 m$, Bl=-2 x $10^3 m$, and Ba=1.1 x $10^3 m$.

Institut des géosciences de l'environnement

Thule domain bedrock topography

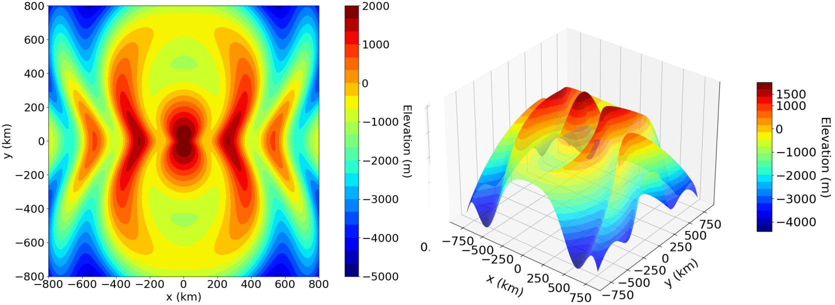

Figure: Thule bedrock topography 3D. On the left side the top view, and on the right side a lateral view.

Thule experimental profiles

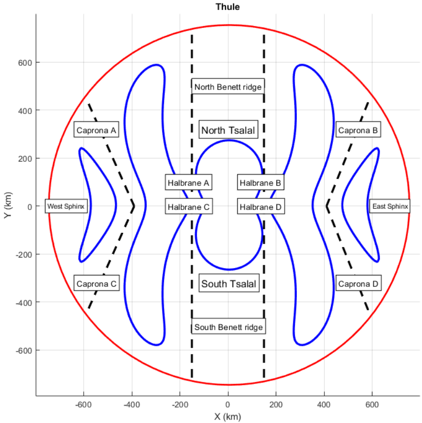

Figure: Thule domain experimental profiles as well as the initial imposed calving front position. Adapted from CalvinMIP inter-comparison project.

Institut des géosciences de l'environnement

Numerical parameters

Table: Physical parameters

Variable	Description	Units
$g = 9.81$	Gravitational acceleration	ms^{-2}
$a_s = 0.3$	Surface mass balance (SMB)	ma^{-1}
$a_b = 0$	Basal mass balance (BMB)	ma^{-1}
$\rho i = 917$	Ice density	$\mathrm{kg\ m}^{-3}$
$\rho w = 1028$	Sea water density	$\mathrm{kg\ m}^{-3}$
$A = 2.9377\mathrm{x}10^{-9}$	Ice rate factor	$\mathrm{KPa}^{-3}\mathrm{a}^{-1}$
$n = 3$	Flow law stress exponent	Dimensionless
$C = 0.001$	basal slipperiness	$\mathrm{ma}^{-1}\mathrm{KPa}^{-3}$
$m = 3$	Sliding law stress exponent	Dimensionless
$s2a = 31556926$	Seconds in a year	s

Numerical variables, external forcings and initial condition

- The numerical resolution will be the variable parameter, varying from 10km, 5km, 2km, and 1km.

Institut
des géosciences
de l'environnement

Numerical variables, external forcings and initial condition

- The numerical resolution will be the variable parameter, varying from 10km, 5km, 2km, and 1km.
- The external forces acting will be gravity, as well as the ice friction and the basal stress.

Institut des géosciences de l'environnement

Numerical variables, external forcings and initial condition

- The numerical resolution will be the variable parameter, varying from 10km, 5km, 2km, and 1km.
- The external forces acting will be gravity, as well as the ice friction and the basal stress.
- The initial condition will be a topography with no ice, namely h_0=0m.

Numerical variables, external forcings and initial condition

- The numerical resolution will be the variable parameter, varying from 10km, 5km, 2km, and 1km.
- The external forces acting will be gravity, as well as the ice friction and the basal stress.
- The initial condition will be a topography with no ice, namely h_0=0m.
- The CFL condition will be necessary to verify the stability of the model. It is needed that:

$$C = \frac{u\Delta t}{\Delta x} < C_{max}; \tag{16}$$

where, C is the Courant number, u is the velocity, Δt is the time step, Δx is the horizontal resolution. $C_{max} = 1$ is a safe approximation.

Institut des géosciences de l'environnement

Results:Cone ice thickness

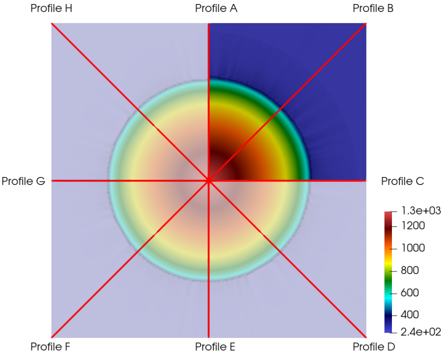

(a) Profiles for Cone circular domain

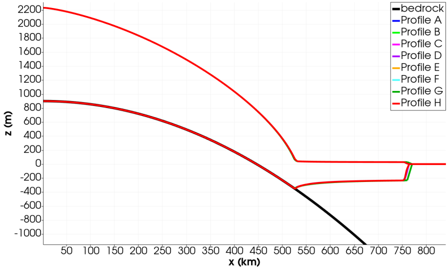

(b) Ice thickess per profile

Figure: Circular domain ice sheet showing the ice thickness results along the profiles proposed.

Volume variation in time and per number of nodes

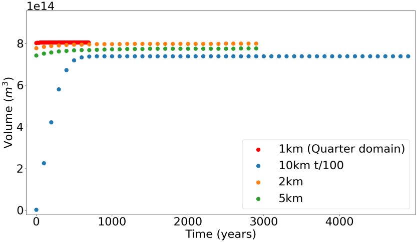

(a) Volume variation in time.

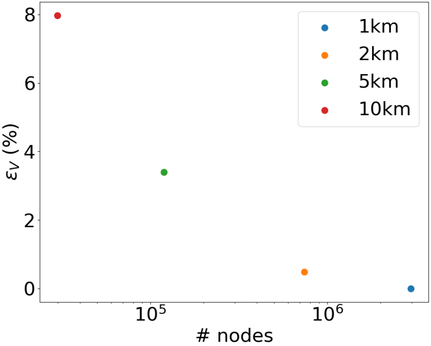

(b) Volume relative variation as a function of the number of nodes.

Figure: Volume variation in time and per number of nodes for the cone experiment.

Simulations time as a function of the number of nodes

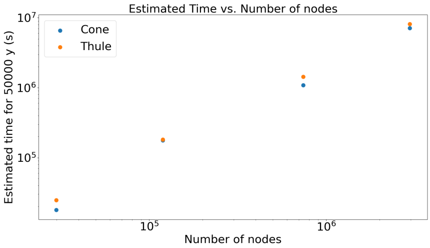

(a) Time for 32 processors used.

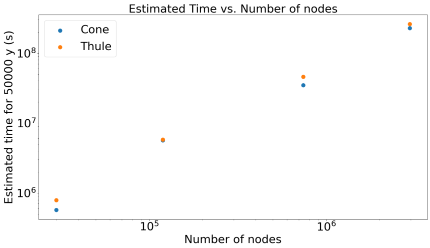

(b) Time for 1 processor.

Figure: Simulation time as a function of the number of nodes for each resolution mesh.

Institut des géosciences de l'environnement

Grounding line position per resolution

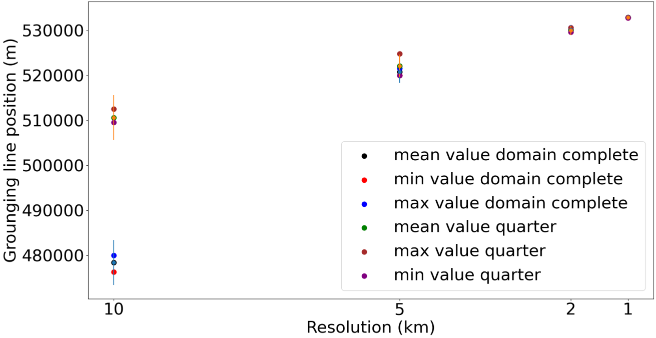

Figure: Grounding line positions as a function of the resolution for quarter and complete circular cone domain.

Results: Thule ice thickness

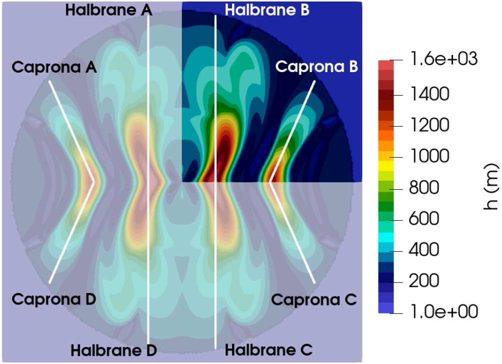

Figure: Ice thickness along the different profiles for the thule domain

Ice thickness along profiles

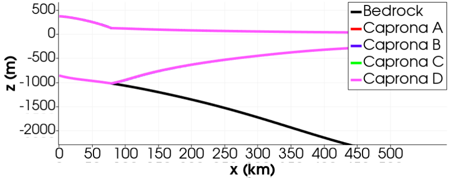

(a) Ice thickness along each Caprona profiles.

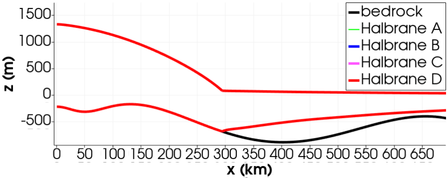

(b) Ice thickness along each Halbrane profiles.

Figure: Ice thickness along the thule domain profiles.

Volume variation in time and per number of nodes

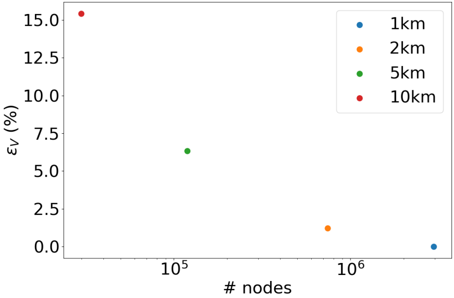

(a) Volume relative variation as a function of the number of nodes.

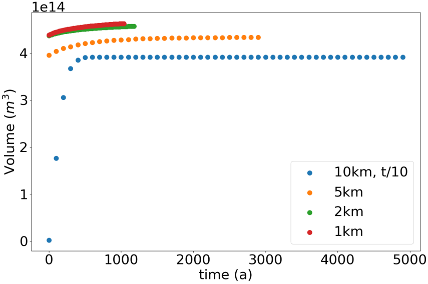

(b) Volume variation in time.

Figure: Volume variation in time and as a function of the number of nodes for the Thule experiment.

IGE
Institut des géosciences de l'environnement

Grounding line position along profiles in Thule

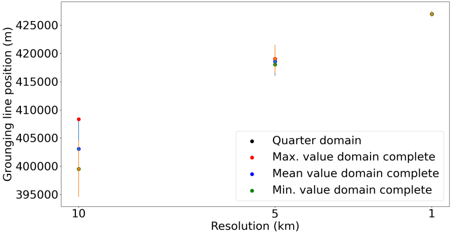

(a) Grounding line positions along Capronas profiles.

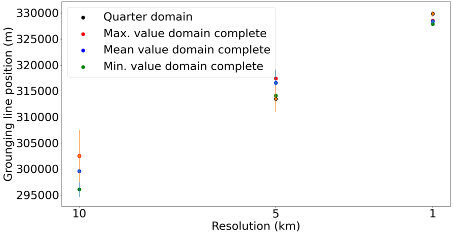

(b) Grounding line positions along Halbrane profiles

Figure: Grounding line positions as a function of the resolution for quarter and complete thule domain along the Caprona and Halbrane profiles.

Conclusions

- The grounding line position is increasing as a function of the resolution, due to the topography of both experiments.

Conclusions

- The grounding line position is increasing as a function of the resolution, due to the topography of both experiments.
- The fact of imposing a calving front, causes that the the ice thickness increases with the resolution, as the flux through the grounding line is increasing, causing that the grounding line position advances.

Institut
des géosciences
de l'environnement

Conclusions

- The grounding line position is increasing as a function of the resolution, due to the topography of both experiments.
- The fact of imposing a calving front, causes that the the ice thickness increases with the resolution, as the flux through the grounding line is increasing, causing that the grounding line position advances.
- The resolution has a direct impact in the symmetry of the domain of study, leading to differences in results of parts of the domain if the resolution is low.

Bibliography and references I

Brunt, K. M., Fricker, H. A., Padman, L., Scambos, T. A., and O'Neel, S. (2010). Mapping the grounding zone of the ross ice shelf, antarctica, using icesat laser altimetry. *Annals of Glaciology*, 51(55):71–79.

Clark, P. U., Church, J. A., Gregory, J. M., and Payne, A. J. (2015). Recent progress in understanding and projecting regional and global mean sea level change. *Current Climate Change Reports*, 1(4):224–246.

Durand, G., Gagliardini, O., Zwinger, T., Le Meur, E., and Hindmarsh, R. C. (2009). Full stokes modeling of marine ice sheets: influence of the grid size. *Annals of Glaciology*, 50(52):109–114.

Fricker, H. A., Coleman, R., Padman, L., Scambos, T. A., Bohlander, J., and Brunt, K. M. (2009). Mapping the grounding zone of the amery ice shelf, east antarctica using insar, modis and icesat. *Antarctic Science*, 21(5):515–532.

IGE
Institut
des géosciences
de l'environnement

Bibliography and references II

Friedl, P., Weiser, F., Fluhrer, A., and Braun, M. H. (2020). Remote sensing of glacier and ice sheet grounding lines: A review. *Earth-Science Reviews*, 201:102948.

Glen, J. (1958). The flow law of ice: A discussion of the assumptions made in glacier theory, their experimental foundations and consequences. *IASH Publ*, 47(171):e183.

Hanna, E., Navarro, F., Pattyn, F., Domingues, C., Fettweis, X., Ivins, E., Nicholls, R., Ritz, C., Smith, B., and Tulaczyk, S. (2013). White-25 house, pl, and zwally, hj: Ice-sheet mass balance and climate change. *Nature*, 498:51–59.

Hooke, R. L. (2019). *Principles of glacier mechanics*. Cambridge university press.

Hutter, K. (1982). A mathematical model of polythermal glaciers and ice sheets. *Geophysical & Astrophysical Fluid Dynamics*, 21(3-4):201–224.

Institut des géosciences de l'environnement

Pritchard, H., Ligtenberg, S. R., Fricker, H. A., Vaughan, D. G., van den Broeke, M. R., and Padman, L. (2012). Antarctic ice-sheet loss driven by basal melting of ice shelves. *Nature*, 484(7395):502–505.

Weertman, J. (1974). Stability of the junction of an ice sheet and an ice shelf. *Journal of Glaciology*, 13(67):3–11.

Institut des géosciences de l'environnement